

---

# Self-setting collagen-calcium phosphate bone cement: Mechanical and cellular properties

---

Jennifer L. Moreau, Michael D. Weir, Hockin H. K. Xu

Department of Endodontics, Prosthodontics and Operative Dentistry, University of Maryland Dental School, 650 West Baltimore Street, Baltimore, Maryland 21201

Received 15 January 2008; revised 18 April 2008; accepted 30 July 2008

Published online 4 November 2008 in Wiley InterScience (www.interscience.wiley.com). DOI: 10.1002/jbm.a.32248

**Abstract:** Calcium phosphate cement (CPC) can conform to complex bone cavities and set *in-situ* to form bioresorbable hydroxyapatite. The aim of this study was to develop a CPC-collagen composite with improved fracture resistance, and to investigate the effects of collagen on mechanical and cellular properties. A type-I bovine-collagen was incorporated into CPC. MC3T3-E1 osteoblasts were cultured. At CPC powder/liquid mass ratio of 3, the work-of-fracture (mean  $\pm$  sd;  $n = 6$ ) was increased from  $(22 \pm 4)$  J/m<sup>2</sup> at 0% collagen, to  $(381 \pm 119)$  J/m<sup>2</sup> at 5% collagen ( $p \leq 0.05$ ). At 2.5–5% of collagen, the flexural strength at powder/liquid ratios of 3 and 3.5 was 8–10 MPa. They matched the previously reported 2–11 MPa of sintered porous hydroxyapatite implants. SEM revealed that the collagen fibers were covered with nano-apatite crystals and bonded to the CPC matrix. Higher collagen content increased the osteoblast cell attachment ( $p \leq 0.05$ ). The

number of live cells per specimen area was  $(382 \pm 99)$  cells/mm<sup>2</sup> on CPC containing 5% collagen, higher than  $(173 \pm 42)$  cells/mm<sup>2</sup> at 0% collagen ( $p \leq 0.05$ ). The cytoplasmic extensions of the cells anchored to the nano-apatite crystals of the CPC matrix. In summary, collagen was incorporated into *in situ*-setting, nano-apatitic CPC, achieving a 10-fold increase in work-of-fracture (toughness) and two-fold increase in osteoblast cell attachment. This moldable/injectable, mechanically strong, nano-apatite-collagen composite may enhance bone regeneration in moderate stress-bearing applications. © 2008 Wiley Periodicals, Inc. J Biomed Mater Res 91A: 605–613, 2009

**Key words:** calcium phosphate bone cement; collagen; cell attachment; cell density; strength; work-of-fracture; bone tissue engineering

---

## INTRODUCTION

Approximately six million bone fractures occurred in the U.S. each year from 1992 to 1994.<sup>1,2</sup> Hydroxyapatite (HA) and other calcium phosphate (CaP) bioceramics are important for hard tissue repair because of their similarity to the apatite in teeth and bones.<sup>3–5</sup> Extensive studies have improved HA-based and other bioceramics with enhanced osteoconductivity and bone-bonding ability.<sup>6–10</sup> CaP cements can be molded and set *in situ* to provide intimate adaptation to the contours of defect surfaces.<sup>11–15</sup> One CaP cement is comprised of a mixture of tetracalcium phosphate [TTCP: Ca<sub>4</sub>(PO<sub>4</sub>)<sub>2</sub>O] and dicalcium phosphate anhydrous (DCPA: CaHPO<sub>4</sub>), and is referred to as CPC.<sup>11</sup> The CPC powder can be mixed with an

aqueous liquid to form a paste that can be sculpted during surgery to conform to the defects in hard tissues. The paste self-hardens to form resorbable HA.<sup>11,16–18</sup> Because of its excellent osteoconductivity and bone replacement capability, CPC is highly promising for a wide range of clinical applications.<sup>16–18</sup> As a result, CPC was approved in 1996 by the Food and Drug Administration for repairing craniofacial defects in humans, thus becoming the first CPC available for clinical use.<sup>18</sup>

However, the brittleness and low strength of CPC limit its use to only non-load-bearing areas. The use of CPC was “limited to the reconstruction of non-stress-bearing bone,”<sup>17</sup> and “none of the indications include significant stress-bearing applications.”<sup>18</sup>

Several methods were used to develop strong and macroporous CPC scaffolds for tissue ingrowth and bone regeneration.<sup>19–22</sup> Absorbable fibers made from a degradable poly(lactide-co-glycolide) copolymer in CPC provided fracture resistance at the early stages of implantation.<sup>21,22</sup> Degradation of the fiber over time could coincide with the ingrowth of bone and a gradual transfer of load from the biomaterial to the natural bone. Another method was the addition of a

Correspondence to: H. H. K. Xu; e-mail: hxu@umaryland.edu

Contract grant sponsor: NIH/NIDCR R01; contract grant number: DE14190

Contract grant sponsor: Maryland Nano-Biotechnology Award; contract grant number: 2007/DBED/UMD Q060101

biopolymer chitosan.<sup>20,22</sup> It was shown that the addition of chitosan and fibers together into CPC had a synergistic reinforcement effect in enhancing the fracture resistance of CPC.<sup>22</sup>

Human bone is comprised of collagen (mainly type I) and nano-sized HA crystals. Hence synthetic HA/collagen composites are promising in mimicking and replacing bone. One study showed that collagen successfully provided a scaffold for bone ingrowth with little evidence of adverse responses.<sup>23</sup> In several previous studies, a collagen network was formed, and then CaP crystals were precipitated onto the outer and inner surfaces of the scaffold.<sup>24–26</sup> In another study, a CaP ceramic was formed first, then a coating of collagen was applied to the surfaces of the ceramic scaffold.<sup>27</sup> In another method, a mixture of CaP/collagen was cold pressed (at a pressure of 150–200 MPa) to remove water and form a solid implant.<sup>23,28</sup> These materials are preforms that require implantation, and they are not moldable or injectable. For a preformed implant such as HA to fit into a bone cavity, the surgeon needs to machine the graft to the desired shape or carve the surgical site around the implant. This increases bone loss, trauma, and surgical time.<sup>29</sup> Only a few studies incorporated collagen into moldable, self-setting CaP cements.<sup>30,31</sup> In one study, collagen decreased the strength of the cement.<sup>30</sup> In another study, collagen decreased the cell activities *in vitro*.<sup>31</sup> Therefore, *in situ*-setting collagen-CaP cement composite with increased cell attachment and improved toughness has yet to be developed.

The objectives of the present study were to: (1) Develop a collagen-CPC composite with improved fracture resistance and increased osteoblast cell attachment; and (2) determine the effects of collagen content on mechanical and cellular properties. The hypothesis was that the incorporation of collagen into CPC would not only increase its fracture resistance, but also enhance its osteoblast cell attachment.

## MATERIALS AND METHODS

### CPC and collagen

The CPC powder consisted of a mixture of tetracalcium phosphate (TTCP,  $\text{Ca}_4(\text{PO}_4)_2\text{O}$ ) and dicalcium phosphate anhydrous (DCPA,  $\text{CaHPO}_4$ ), with a TTCP:DCPA molar ratio of 1:1. TTCP powder was synthesized from a solid-state reaction between  $\text{CaHPO}_4$  and calcium carbonate ( $\text{CaCO}_3$ ) (Baker Chemical Company, NJ), then ground and sieved to obtain TTCP particle sizes of 1–80  $\mu\text{m}$ , with a median particle size of 17  $\mu\text{m}$ . The DCPA powder was ground and sieved to obtain particle sizes of 0.4–3  $\mu\text{m}$ , with a median of 1  $\mu\text{m}$ . The TTCP and DCPA powders were mixed in a blender (Dynamics, New Hartford, CT) to form the CPC powder.

A type I bovine collagen powder (Sigma, St. Louis, MO) was added to CPC to develop an *in situ*-setting, bone-mimicking, nano apatite-collagen composite. According to the manufacturer, cattle Achilles tendon was cleaned of all noncollagenous tissue and extracted at a temperature of 0°C with a 3%  $\text{Na}_2\text{HPO}_4$  solution to remove soluble proteins. To remove mucopolysaccharides, the tendon was extracted with a 25% potassium chloride solution. The resultant collagen was washed with water, dehydrated with absolute alcohol, and air dried. The as-received collagen was in the form of elongated, flexible bundles, with a bundle diameter ranging from approximately 0.1–3  $\mu\text{m}$ . The length of the bundles ranged from about 20–100  $\mu\text{m}$ , although the exact length was difficult to measure because the collagen bundles were flexible and zigzag, and they entangled with each other.

### Specimen fabrication

The CPC powder was mixed with distilled water to form a paste. The collagen powder was mixed with the CPC paste. The following mass fractions of collagen/(collagen + CPC) were used: 0%, 2.5%, and 5.0%. Collagen mass fractions of 7.5% or higher were not included because the collagen fibers entangled and agglomerated. This made the mixing more difficult, and the paste at a CPC powder/liquid mass ratio of 3.5 becoming too dry. The CPC powder/liquid mass ratio,  $P/L$ , was 3.5/1, 3.0/1, and 2.5/1.  $P/L$  mass ratio of 4 (4 is equivalent to 4/1) or higher was not tested because the CPC-collagen paste was too dry.  $P/L$  mass ratio of 2 or lower was not tested because the set cement was too weak mechanically. The mixed CPC-collagen paste was placed into molds of 3 mm  $\times$  4 mm  $\times$  25 mm. Each specimen was set in a humidifier with 100% relative humidity at 37°C for 4 h, and then demolded and immersed in distilled water at 37°C for 24 h prior to testing.

### Mechanical testing

A 3  $\times$  3 full factorial design was tested, with three levels of collagen mass fraction (0%, 2.5%, and 5%), and three levels of  $P/L$  ratio (2.5, 3.0, 3.5). A three-point flexural test<sup>32</sup> with a span of 20 mm was used to fracture the specimens at a crosshead speed of 1 mm per minute on a computer-controlled Universal Testing Machine (model 5500R, MTS, Cary, NC). Flexural strength was calculated by  $S = 3 F_{\text{max}} L / (2 b h^2)$ , where  $F_{\text{max}}$  is the maximum load on the load-displacement curve,  $L$  is flexure span,  $b$  is specimen width, and  $h$  is specimen thickness. Elastic modulus was calculated by  $E = (F/c) (L^3 / [4 b h^3])$ , where load  $F$  divided by the corresponding displacement  $c$  is the slope of the load-displacement curve in the linear elastic region. Work-of-fracture, or toughness, is the energy required to fracture the specimen. This was obtained from the area under the load-displacement curve divided by the specimen's cross-sectional area.<sup>13</sup> After the matrix had cracked, many of the composite specimens were still intact because of the collagen fibers bridging the cracks and supporting the applied load. The test was stopped at a maximum crosshead dis-

placement of 1 mm for a consistent calculation of work-of-fracture.

### CPC conversion to HA

Powder X-ray diffraction (XRD) was used to examine the CPC conversion to HA. CPC-collagen specimens were ground into a powder in acetone to remove the water using a mortar and pestle. The XRD patterns were recorded with a powder X-ray diffractometer (Rigaku, Danvers, MA) with the use of graphite-monochromatized copper K $\alpha$  radiation ( $\lambda = 0.154$  nm) generated at 40 kV and 40 mA. The 002 peak intensity of HA was used to measure the percentage of conversion to HA. All data were collected in a continuous scan mode ( $1^\circ 2\theta \text{ min}^{-1}$ , step time 0.6 s, step size  $0.01^\circ$ ).

### Cell culture

CPC composite specimens were fabricated using  $3 \times 4 \times 25$  mm molds for materials with collagen volume fractions of 0%, 2.5%, and 5% at a cement powder/liquid ratio of 3.5, selected because of the relatively high mechanical strength. The set specimens were sterilized in an ethylene oxide sterilizer (Anprolene AN 74i, Andersen, Haw River, NC) for 12 h according to the manufacturer's specifications. The specimens were then degassed for at least 7 days to remove any remaining ethylene oxide gas, and rinsed in Dulbecco's phosphate buffer saline (PBS, Gibco, Rockville MD) before beginning the cell experiment.

Clonal murine calvarial cells, MC3T3-E1 subclone 4 (American Type Culture, Manassas, VA), were cultured following established protocols.<sup>33,34</sup> Cells were cultured in flasks at 37 °C and 100% humidity with 5% CO<sub>2</sub> in  $\alpha$ -modified Eagle's minimum essential medium ( $\alpha$ -MEM, Cambrex Bio Science, Walkersville, MD). The medium was supplemented with 10% volume fraction fetal bovine serum (FBS, Gibco), 1% penicillin/streptomycin, 1% L-glutamine, and 1% sodium pyruvate (Cambrex). The medium was changed every two days. The cultures were passaged with trypsin when confluent. Fifty thousand cells diluted into 2 mL of media were added to each well containing a specimen, and incubated for 1 day.<sup>32-34</sup>

After 1-day incubation, the media was removed and the cells were washed with 2 mL of PBS. Cell viability was assessed using the live/dead viability/cytotoxicity kit (Molecular Probes, Eugene, OR). Each specimen was incubated for 10 min at 37°C with 2 mL of  $\alpha$ -MEM containing 4  $\mu\text{M}$  calcein-AM and 2  $\mu\text{M}$  ethidium homodimer-1 to stain live and dead cells, respectively. Cells were then viewed by epifluorescence microscopy (TE300, Nikon, Melville, NY). Photos of the cells were obtained with a digital camera (Cool Pix 990, Nikon, Melville, NY).

Two parameters were measured. First, the percent of live cells was measured. Two randomly chosen fields of view were photographed from each specimen. Each field of view was photographed after selecting the proper filter for calcein-AM and ethidium homodimer-1, respectively, to yield five pictures from each specimen. Five specimens were examined for each of the three materials above. Each

of the images was printed and the cells were counted.<sup>34</sup>  $N_{\text{Live}}$  is the number of live cells in the image and  $N_{\text{Dead}}$  is the number of dead cells in the image.  $P_{\text{Live}}$  = The percent of live cells. Hence,  $P_{\text{Live}} = N_{\text{Live}} / (N_{\text{Live}} + N_{\text{Dead}})$ .

The second parameter was the cell attachment on CPC composite,  $C_{\text{Attach}}$ .  $C_{\text{Attach}}$  is defined as the number of live cells attached on the specimen in the view field divided by the area ( $A$ ) of the view field:  $C_{\text{Attach}} = N_{\text{Live}} / A$ . Both  $P_{\text{Live}}$  and  $C_{\text{Attach}}$  are measured because a high value of  $P_{\text{Live}}$  only means that there are few dead cells. It does not necessarily mean a large number of live cells that are attached onto the specimens.  $C_{\text{Attach}}$  quantifies the absolute number of live cells anchored on the specimen per surface area.

### Scanning electron microscopy and statistics

A scanning electron microscope (SEM, model JSM-5300, JEOL, Peabody, MA) was used to observe both collagen fibers and the fractured surfaces of the specimens. The specimens were sputter coated with gold prior to SEM observations.

One-way and two-way analyses of variance (ANOVA) were performed to detect significant effects in the data. Tukey's multiple comparison procedures were used to compare the data at a family confidence coefficient of 0.95.

## RESULTS

Figure 1 plots mechanical properties versus collagen mass fraction for the CPC-collagen composite. Two-way ANOVA showed significant effects of collagen content and powder/liquid ( $P/L$ ) mass ratio, with a significant interaction between the two parameters ( $p \leq 0.05$ ). In Figure 1(A), at  $P/L$  of 3.5, flexural strength (mean  $\pm$  sd;  $n = 6$ ) significantly decreased from  $(13.9 \pm 2.3)$  MPa at 0% collagen to  $(9.0 \pm 2.5)$  MPa at 5% collagen ( $p \leq 0.05$ ). However, at a  $P/L$  mass ratio of 3 and 2.5, collagen mass fraction had no significant effect on flexural strength ( $p > 0.1$ ).

Elastic modulus [Fig. 1(B)] significantly decreased from  $(7.7 \pm 1.0)$  GPa at 0% collagen to  $(5.2 \pm 1.3)$  GPa at 5% collagen ( $p \leq 0.05$ ). Collagen content had no significant effects on modulus at  $P/L$  of 3 and 2.5. At 0% collagen, elastic modulus of  $(7.7 \pm 1.0)$  GPa at  $P/L$  of 3.5 was significantly higher than  $(5.1 \pm 0.9)$  GPa at  $P/L$  of 2.5 ( $p \leq 0.05$ ).

Figure 2(A) shows typical load-displacement curves. CPC without collagen failed in a brittle manner. CPC with 5% collagen failed noncatastrophically. The work-of-fracture [Fig. 2(B)] was increased from  $(9.4 \pm 3.1)$  J/m<sup>2</sup> with 0% collagen to  $(430 \pm 103)$  J/m<sup>2</sup> with 5% collagen ( $p \leq 0.05$ ) at a  $P/L$  ratio of 2.5. At  $P/L$  of 3, the work-of-fracture was increased from  $(22.2 \pm 3.8)$  J/m<sup>2</sup> without collagen, to  $(381 \pm 119)$  J/m<sup>2</sup> with 5% collagen ( $p \leq 0.05$ ).

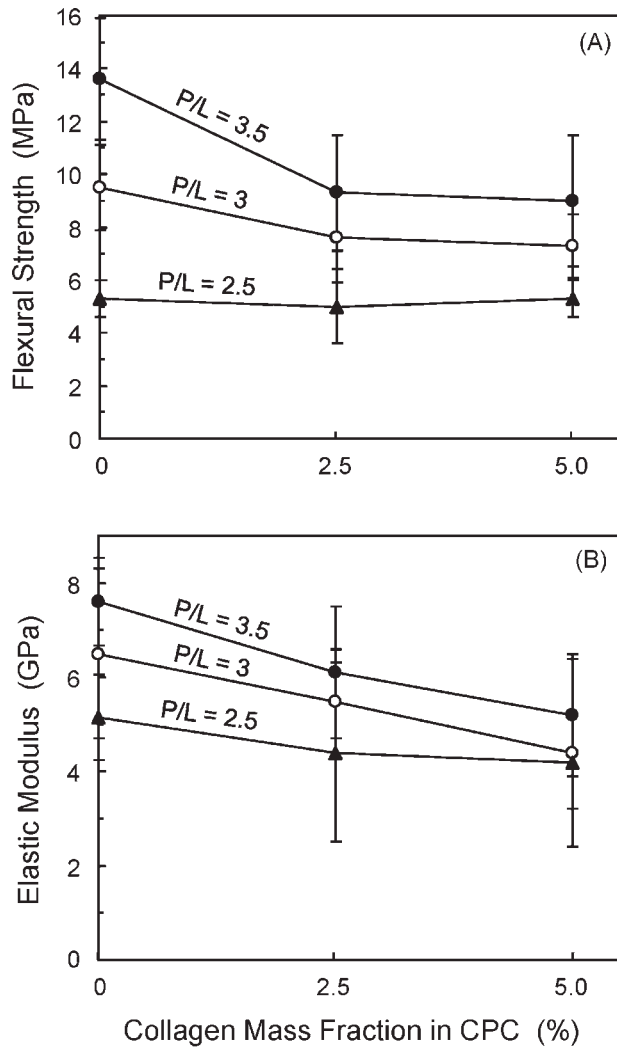
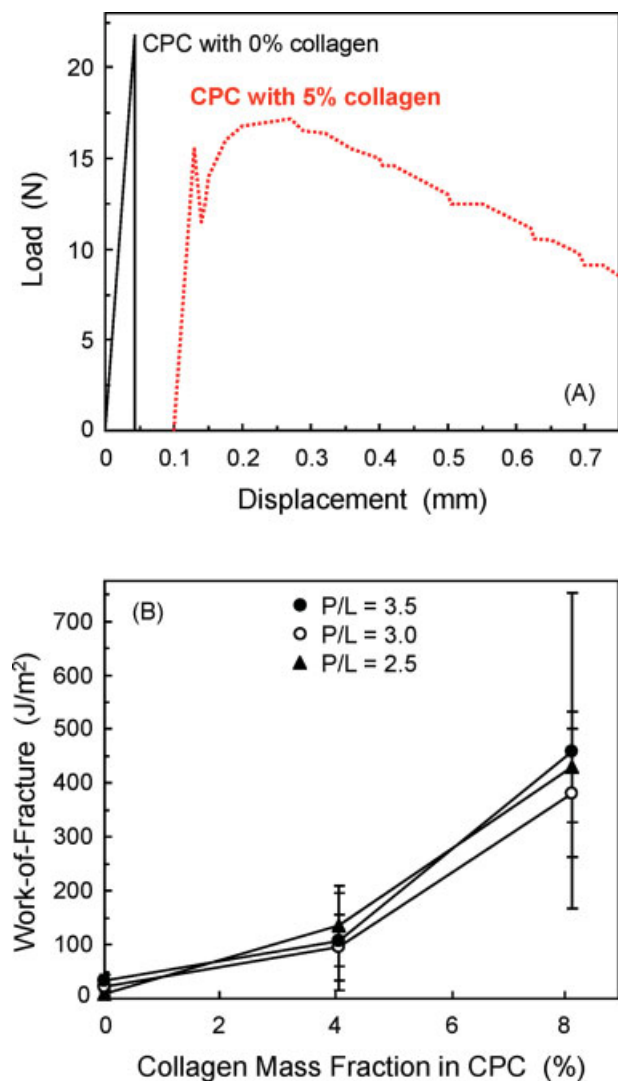


**Figure 1.** Flexural strength and elastic modulus of CPC vs. collagen content. Each value is the mean of six measurements with the error bar showing one standard deviation (mean  $\pm$  sd;  $n = 6$ ).

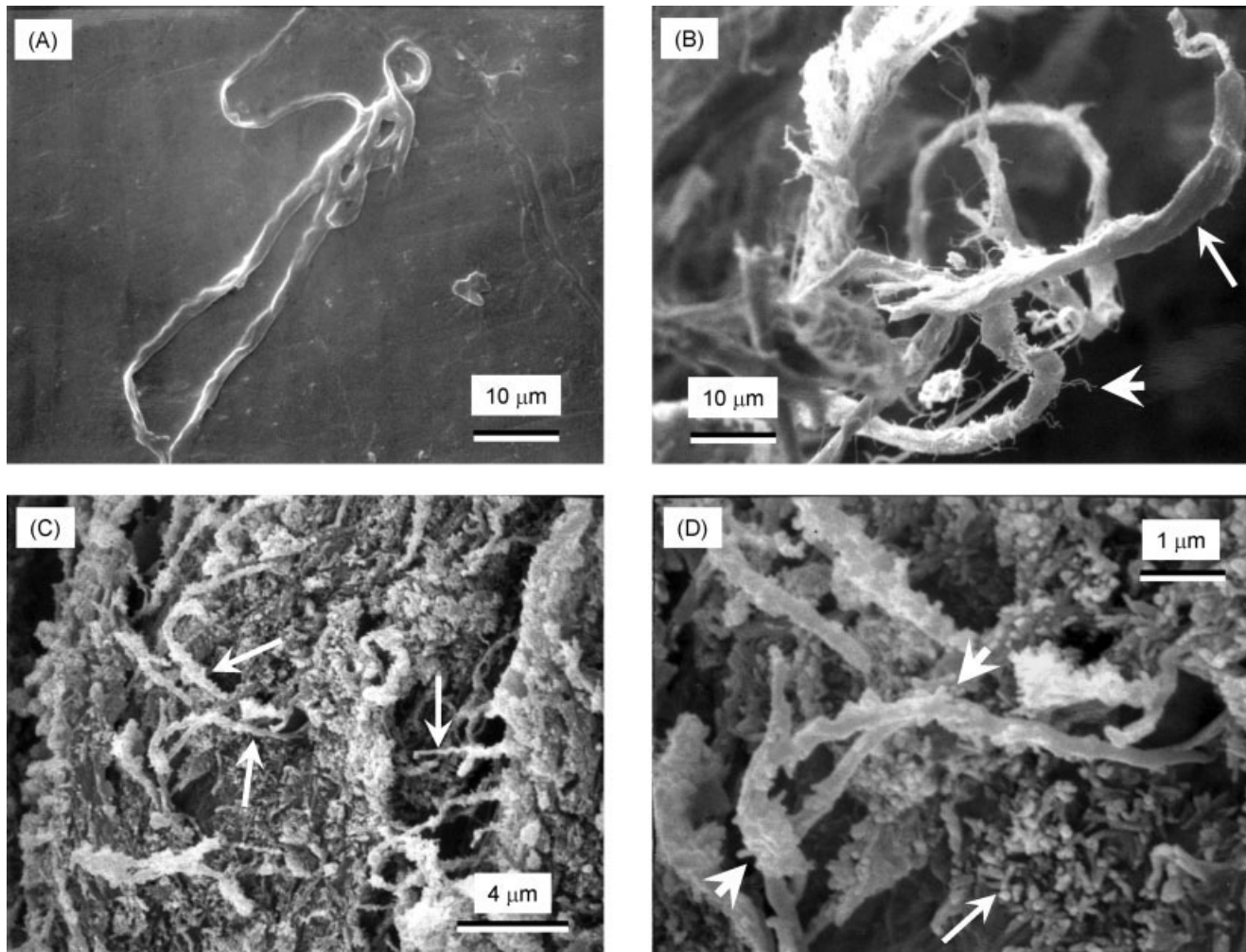
Regarding the mass percent of CPC conversion to HA, two-way ANOVA showed significant effects of collagen mass fraction and  $P/L$  mass ratio, with a significant interaction between the two variables ( $p \leq 0.05$ ). At  $P/L$  of 3.5, the HA conversion (mean  $\pm$  sd;  $n = 3$ ) decreased from ( $73.4 \pm 6.3$ )% for CPC containing 0% collagen to ( $57.6 \pm 1.4$ )% with 5% volume fraction of collagen ( $p \leq 0.05$ ). At  $P/L$  of 2.5, the HA conversion decreased from ( $79.4 \pm 1.2$ )% at 0% collagen to ( $59.5 \pm 7.5$ )% at 5% collagen ( $p \leq 0.05$ ). The HA conversion percentile at an intermediate  $P/L$  of 3 was in between those at  $P/L$  of 3.5 and 2.5.

An example of the as-received collagen fiber bundle is shown in Figure 3(A). Figure 3(B) shows pulled-out collagen fibers on a specimen fracture surface at  $P/L$  of 3.5 with 5% collagen. Small fibrils (short arrow in B) are visible separating from the

bundle (long arrow), consistent with the fact that the collagen bundles were made by braiding the individual collagen fibrils together. This braided structure gave the bundle a relatively rough and tortuous surface, with enhanced mixing with the CPC paste and interlocking of the fibers in the set matrix. Figure 3(C) shows collagen fibers (arrows) covered with the small HA crystals that make up the CPC matrix. At a high magnification in Figure 3(D), the long arrow indicates examples of the nano HA crystals in the CPC matrix. The HA crystals had a thickness of approximately 50–100 nm, and a length of about 100–300 nm. The short arrows point to collagen fibers coated with nano HA crystals, indicating an intimate contact between collagen fibers and HA crystals.



**Figure 2.** (A) Typical load-displacement curves of CPC specimens with 0% and 5% collagen. (B) Work-of-fracture (mean  $\pm$  sd;  $n = 6$ ) of CPC composite as a function of collagen content. [Color figure can be viewed in the online issue, which is available at [www.interscience.wiley.com](http://www.interscience.wiley.com).]



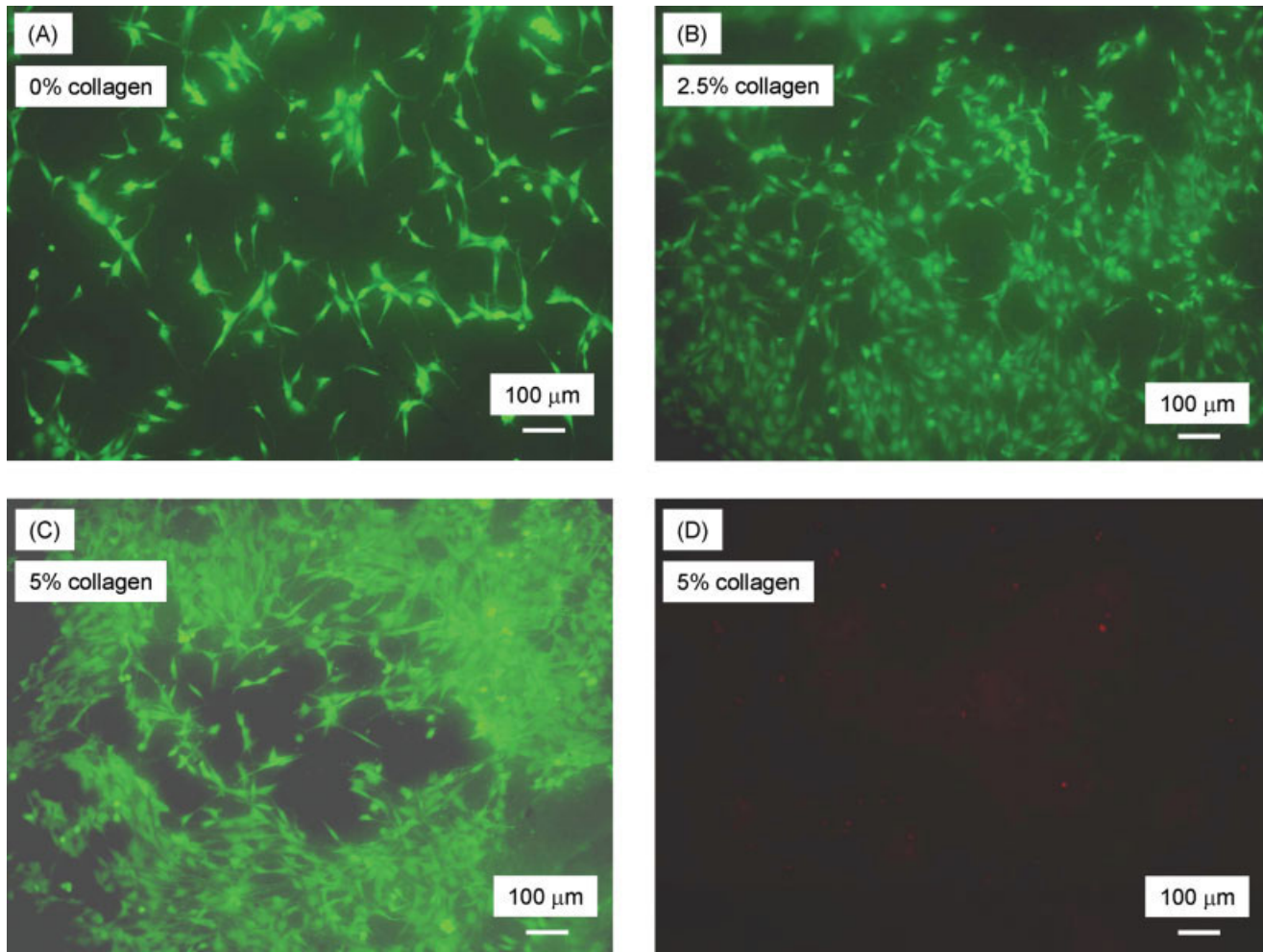
**Figure 3.** SEM of: (A) As-received collagen fiber bundle. (B) Pulled-out collagen fibers on a specimen fracture surface at powder/liquid ratio  $P/L$  of 3.5 with 5% collagen. Small fibrils are visible separating from the bundle (long arrow). (C) Collagen fibers (arrows) covered with the nano HA crystals that make up the CPC matrix. (D) At a higher magnification, nano HA crystals in the CPC matrix had intimate contact with collagen fibers.

Figure 4 shows cells cultured for 1 day on CPC-collagen composite with (A) 0% collagen, (B) 2.5% collagen, and (C) 5% collagen, all at  $P/L$  of 3.5. Live cells, stained green, appeared to have adhered and attained a normal polygonal morphology on the specimens. Increasing the collagen content increased the number of cells attached to the composite. Dead cells were very few; an example of this is shown in Figure 4(D) for CPC with 5% collagen.

The above cell attachment behavior was quantified and plotted in Figure 5(A), where the number of live cells was measured per specimen surface area. Increasing the collagen mass fraction significantly increased the number of cell attachment per specimen area ( $p \leq 0.05$ ). The number of live cells/specimen area was  $(382 \pm 99)$  cells/mm<sup>2</sup> at 5% collagen, significantly higher than  $(173 \pm 42)$  cells/mm<sup>2</sup> at 0% collagen ( $p \leq 0.05$ ). Because of the low numbers of

dead cells, the percentages of live cells were high, ranging from 94 to 96% [Fig. 5(B)].

Figure 6(A) shows a SEM photo of an osteoblast cell (O) cultured for 1 day on CPC with 0% collagen. The cell developed cytoplasmic extensions (E) with lengths of 20–30  $\mu\text{m}$  that anchored on CPC. These cytoplasmic extensions are regions of the cell plasma membrane that contain a meshwork or bundles of actin-containing microfilaments which permit the movement of the migrating cells along a substratum.<sup>35</sup> In (B), cell 1 and cell 2 had formed cell–cell junctions (J) and developed extensions that bridged a pore in the surface of CPC-collagen composite at 2.5% of collagen. In (C), the cells had resided into a pore in CPC-collagen composite with 5% collagen. The tip of the cytoplasmic extension indicated by the arrow in (C) is shown at a high magnification in (D), showing that it was firmly attached to the HA crystals.



**Figure 4.** Cells cultured for 1 day: (A) live cells (stained green) on CPC specimens with 0% collagen, (B) live cells on CPC specimens with 2.5% collagen, (C) live cells on CPC specimens with 5% collagen, and (D) dead cells (stained red) on CPC with 5% collagen. [Color figure can be viewed in the online issue, which is available at [www.interscience.wiley.com](http://www.interscience.wiley.com).]

## DISCUSSION

A nano apatite-collagen composite is an ideal scaffold or matrix for bone tissue engineering because it has the major components of the extracellular matrix (ECM) of bone. Collagen provides support to connective tissues such as bones, cartilage, skin, tendons, ligaments, and blood vessels.<sup>36,37</sup> Type I collagen is commonly used as a tissue culture substrate, but has also been used as a biomaterial in applications such as an injectable collagen for soft tissue augmentation, hemostats, wound dressings, and vascular graft coatings.<sup>36–38</sup>

### Mechanical properties

Researchers developed collagen matrices with different porosities and reinforced with synthetic polymers such as poly(glycolic acid) or poly(lactide-co-glycolide) fibers.<sup>39,40</sup> Another approach to incorpo-

rating collagen into tissue engineering systems was through coating the biomaterial surface with collagen.<sup>41</sup> Other researchers created collagen-HA composites through solid free-form fabrication,<sup>42</sup> or through homogenous mixing of HA and type I collagen.<sup>25</sup> These collagen-containing biomaterials are either prefabricated and not moldable/injectable nor capable of hardening *in situ*, or they have inadequate fracture resistance or geometrical stiffness.

The present study differs from these previous studies because the nano apatite-collagen composite was moldable, *in situ*-hardening, and with a relatively high fracture resistance. For the purpose of comparison, the previously-reported flexural strengths of commercial sintered porous HA implants ranged from 2 to 11 MPa,<sup>4</sup> and cancellous bone had a tensile strength of 3.5 MPa. The new collagen-CPC composite at powder:liquid ratios of 3 and 3.5, with 2.5% and 5% collagen, had flexural strengths of 8 to 10 MPa. The advantage of the new nano-apatite collagen scaffold is that it is moldable

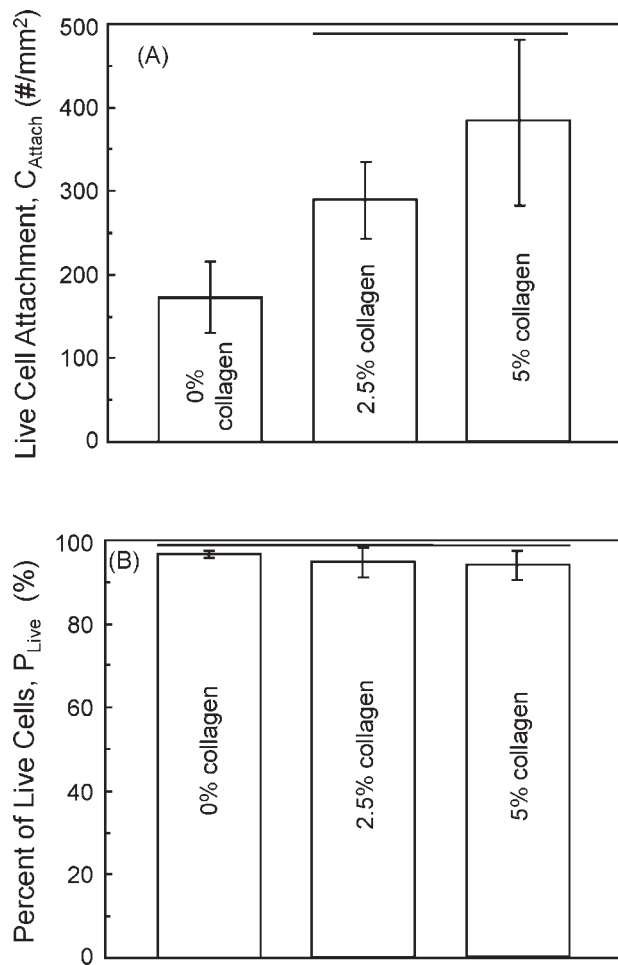


**Figure 5.** (A) Live cell attachment = Number of live cells/mm<sup>2</sup> of CPC specimen surface area (mean  $\pm$  sd;  $n = 5$ ). Horizontal lines indicate values that are not significantly different (Tukey's multiple comparison test; family confidence coefficient = 0.95). (B) Live cell density = Number of live cells/(number of live cells + number of dead cells). Horizontal lines indicate values that are not significantly different (Tukey's at 0.95).

and can set *in-situ*, resulting in intimate adaptation to complex bone cavities without machining. Furthermore, CPC is resorbable, while sintered HA is relatively stable *in vivo*. For another comparison, a composite scaffold based on collagen co-electrospun with nano HA exhibited a tensile strength of 1.68 MPa.<sup>43</sup> Even accounting for the possible differences because of the different testing methods, the 8–10 MPa of the new CPC-collagen composite was significantly higher. Besides a relatively high strength, the toughness (work-of-fracture) of the CPC-collagen composite showed a 10-fold increase (Fig. 2). Several mechanisms have contributed to this improvement. Arrows in Figure 3(C) indicate areas of the fracture surface where fiber pullout from the CPC matrix occurred, a mechanism that consumes energy and contributes to the fracture resistance in many com-

posite materials. Figure 3(D) shows nano-sized HA crystals deposited on the collagen fibril surface, indicating intimate incorporation of collagen with the CPC paste and the ability of nano HA to precipitate and grow on the collagen fibers. This may have increased the efficacy of crack bridging, the resistance to crack propagation and the friction in fiber pullout.

### Cellular properties

Cell adhesion to extracellular matrices is essential to the development, maintenance, and remodeling of osseous tissues. Adhesive interactions play a critical role in osteoblast survival, proliferation, differentiation, and matrix mineralization. These interactions also play a part in bone formation, osteoclast function, and bone resorption.<sup>44</sup> Previous studies have measured osteoblast interactions with prefabricated CaP ceramics coated with type I collagen, and found that proliferation proceeded more rapidly on materials coated with collagen than on uncoated materials.<sup>27</sup> However, the present study was the first to show that collagen incorporation into a self-setting CPC not only increased its work-of-fracture by an order of magnitude, but also doubled its osteoblast cell attachment.

The live cell attachment was significantly higher on scaffolds with 2.5% and 5% collagen, compared to that with 0% collagen. Figure 6 showed that cells attached to the CPC-collagen composite and exhibited a healthy polygonal morphology with cytoplasmic extensions firmly attached to nano HA crystals. Type I collagen contains the Asp-Gly-Glu-Ala (DGEA) amino acid sequence that mediates cell binding via integrin receptors.<sup>45,46</sup> The cell attachment protein fibronectin is also important in promoting binding of cells to collagen. Because of these interactions, collagen-containing scaffolds present a more native surface to cells relative to synthetic polymer or inorganic scaffolds for tissue engineering.<sup>45</sup> The nano apatite-collagen composite of the present study is more biomimetic and more similar to natural bone than the nano apatite cement without collagen, consistent with a substantially increased attachment of the number of live cells [Fig. 5(A)]. Further studies are needed to examine the performance of the new collagen-CPC composite in animal models.

### SUMMARY

Self-hardening, CPC-collagen composite was developed with a 10-fold increase in work-of-fracture (toughness) and two-fold increase in osteoblast

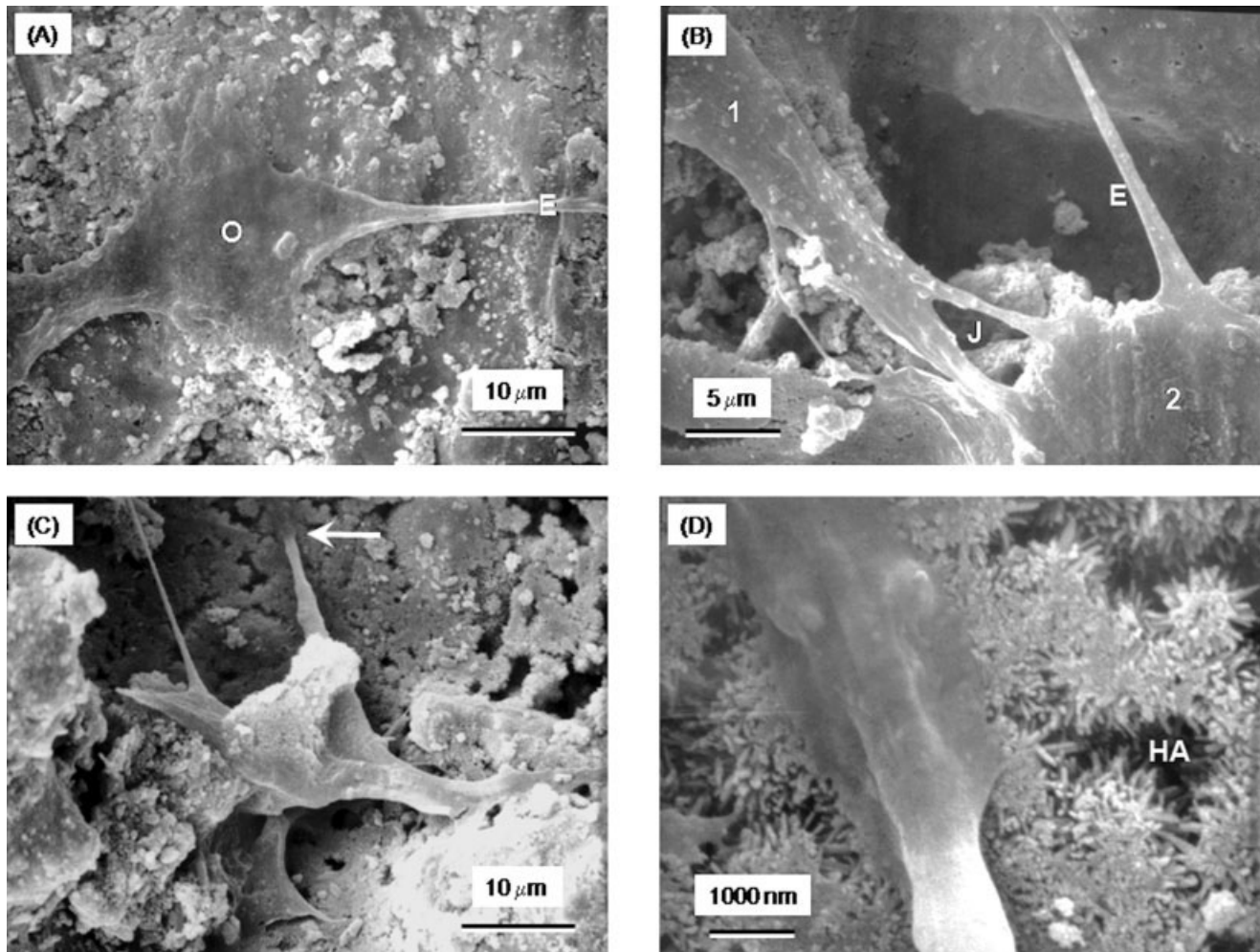


**Figure 6.** (A) SEM of an osteoblast cell (O), and cytoplasmic extensions (E), on CPC control with 0% collagen. (B) Cell-cell junctions (J) between cells and extensions that bridged a pore in the CPC-collagen composite at 2.5% collagen. (C) Cells residing in a pore in CPC-collagen composite with 5% collagen. (D) Higher magnification of feature in (C) showing the tip of the cytoplasmic extension and its firm attachment to the nano HA crystals.

cell attachment. The nano apatite-collagen composite had flexural strengths of 8–10 MPa. These values matched the previously reported 2 to 11 MPa flexural strength of commercial sintered porous HA implants. The new composite can be molded to the desired shape and set *in-situ* to conform to complex bone cavities with intimate adaptation to neighboring bone. This relatively strong collagen-CPC composite may be useful for bone tissue engineering in moderate load-bearing as well as nonload-bearing applications, with a biomimetic, nano apatite-collagen matrix to enhance cellular attachment and bone regeneration.

We thank Drs. S. Takagi and L. C. Chow at the Paffenbarger Research Center and Dr. Carl G. Simon at the National Institute of Standards and Technology for discussions and help.

## References

1. Praemer A, Furner S, Rice DP. Musculoskeletal conditions in the United States. Rosemont: Am Acad Orthop Surg 1999, Foreword, p IX.
2. Medical Data International. RP-651147—Orthopedic and musculoskeletal markets: Biotechnology and tissue engineering. 2000:28–31.
3. LeGeros RZ. Biodegradation and bioresorption of calcium phosphate ceramics. *Clin Mater* 1993;14:65–88.
4. Suchanek W, Yoshimura M. Processing and properties of hydroxyapatite-based biomaterials for use as hard tissue replacement implants. *J Mater Res* 1998;13:94–117.
5. Hing KA, Best SM, Bonfield W. Characterization of porous hydroxyapatite. *J Mater Sci: Mater Med* 1999;10:135–145.
6. Hench LL. Bioceramics. *J Am Ceram Soc* 1998;81:1705–1728.
7. Ducheyne P, Qiu Q. Bioactive ceramics: The effect of surface reactivity on bone formation and bone cell function. *Biomaterials* 1999;20:2287–2303.
8. Pilliar RM, Filiaggi MJ, Wells JD, Grynblas MD, Kandel RA. Porous calcium polyphosphate scaffolds for bone substitute applications—In vitro characterization. *Biomaterials* 2001;22:963–972.

9. Chu TMG, Orton DG, Hollister SJ, Feinberg SE, Halloran JW. Mechanical and in vivo performance of hydroxyapatite implants with controlled architectures. *Biomaterials* 2002;23:1283–1293.
10. Russias J, Saiz E, Deville S, Gryn K, Liu G, Nalla RK, Tomsia AP. Fabrication and in vitro characterization of three-dimensional organic/inorganic scaffolds by robocasting. *J Biomed Mater Res A* 2007;83:434–445.
11. Brown WE, Chow LC. A new calcium phosphate water setting cement. In: Brown PW, editor. *Cements Research Progress*. Westerville, OH: American Ceramics Society; 1986. pp 352–379.
12. Ginebra MP, Fernandez E, De Maeyer EAP, Verbeeck RMH, Boltong MG, Ginebra J, Driessens FCM, Planell JA. Setting reaction and hardening of an apatite calcium phosphate cement. *J Dent Res* 1997;76:905–912.
13. Durucan C, Brown PW. Low temperature formation of calcium-deficient hydroxyapatite-PLA/PLGA composites. *J Biomed Mater Res* 2000;51:717–725.
14. Barralet JE, Gaunt T, Wright AJ, Gibson IR, Knowles JC. Effect of porosity reduction by compaction on compressive strength and microstructure of calcium phosphate cement. *J Biomed Mater Res B* 2002;63:1–9.
15. Bohner M, Baroud G. Injectability of calcium phosphate pastes. *Biomaterials* 2005;26:1553–1563.
16. Shindo ML, Costantino PD, Friedman CD, Chow LC. Facial skeletal augmentation using hydroxyapatite cement. *Arch Otolaryngol Head Neck Surg* 1993;119:185–190.
17. Friedman CD, Costantino PD, Takagi S, Chow LC. Bone-Source hydroxyapatite cement: A novel biomaterial for craniofacial skeletal tissue engineering and reconstruction. *J Biomed Mater Res* 1998;43:428–432.
18. Chow LC. Calcium phosphate cements: Chemistry, properties, and applications. *Mater Res Symp Proc* 2000;599:27–37.
19. Xu HHK, Quinn JB, Takagi S, Chow LC, Eichmiller FC. Strong and macroporous calcium phosphate cement: Effects of porosity and fiber reinforcement on mechanical properties. *J Biomed Mater Res* 2001;57:457–466.
20. Xu HHK, Quinn JB, Takagi S, Chow LC. Processing and properties of strong and non-rigid calcium phosphate cement. *J Dent Res* 2002;81:219–224.
21. Xu HHK, Quinn JB. Calcium phosphate cement containing resorbable fibers for short-term reinforcement and macroporosity. *Biomaterials* 2002;23:193–202.
22. Xu HHK, Quinn JB, Takagi S, Chow LC. Synergistic reinforcement of in situ hardening calcium phosphate composite scaffold for bone tissue engineering. *Biomaterials* 2004;25:1029–1037.
23. Tenhuisen KS, Martin RI, Klimkiewicz M, Brown PW. Formation and properties of a synthetic bone composite: Hydroxyapatite-collagen. *J Biomed Mater Res* 1995;29:803–810.
24. Du C, Cui FZ, Zhu XD, de Groot K. Three-dimensional nano-HAp/collagen matrix loading with osteogenic cells in organ culture. *J Biomed Mater Res* 1999;44:407–415.
25. Lickorish D, Ramshaw JA, Werkmeister JA, Glattauer V, Howlett CR. Collagen-hydroxyapatite composite prepared by biomimetic process. *J Biomed Mater Res A* 2004;68:19–27.
26. Zou C, Weng WJ, Deng XL, Cheng K, Liu XG, Du PY, Shen G, Han GR. Preparation and characterization of porous beta-tricalcium phosphate collagen composites with an integrated structure. *Biomaterials* 2005;26:5276–5284.
27. Brodie JC, Goldie E, Connel G, Merry J, Grant MH. Osteoblast interactions with calcium phosphate ceramics modified by coating with type I collagen. *J Biomed Mater Res A* 2005;73:409–421.
28. Kikuchi M, Itoh S, Ichinose S, Shinomiya K, Tanaka J. Self-organization mechanism in a bone-like hydroxyapatite/collagen nanocomposite synthesized in vitro and its biological reaction in vivo. *Biomaterials* 2001;22:1705–1711.
29. Laurencin CT, Ambrosio AMA, Borden MD, Cooper JA. Tissue engineering: Orthopedic applications. *Ann Rev Biomed Eng* 1999;1:19–46.
30. Miyamoto Y, Ishikawa K, Takechi M, Toh T, Yuasa T, Nagayama M, Suzuki K. Basic properties of calcium phosphate cement containing atelocollagen in its liquid or powder phases. *Biomaterials* 1998;19:707–715.
31. Hempel U, Reinstorf A, Poppe M, Fischer U, Gelinsky M, Pompe W, Wenzel KW. Proliferation and differentiation of osteoblasts on Biocement D modified with collagen type I and citric acid. *J Biomed Mater Res B* 2004;71:130–143.
32. American Society for Testing and Materials. ASTM D 790–03: Standard test methods for flexural properties of unreinforced and reinforced plastic and electrical insulating materials. West Conshohocken, PA: ASTM International; 2004.
33. Xu HHK, Simon CG Jr. Fast setting calcium phosphate-chitosan scaffold: Mechanical properties and biocompatibility. *Biomaterials* 2005;26:1337–1348.
34. Xu HHK, Carey LE, Simon CG Jr, Takagi S, Chow LC. Pre-mixed calcium phosphate cements: Synthesis, physical properties, and cell cytotoxicity. *Dent Mater* 2007;23:433–441.
35. Lodish H, Berk A, Zipursky SL, Matsudaira P, Baltimore D, Darnell J. *Molecular Cell Biology*, 4th ed. New York: Freeman and Company; 2000. Chapters 18–19.
36. Yang C, Hillas PJ, Baez JA, Nokelainen M, Balan J, Tang J, Spiro R, Polarek JW. The application of recombinant human collagen in tissue engineering. *BioDrugs* 2004;18:103–119.
37. Kleinman HK, Luckenbill-Edds L, Cannon FW, Sephel GC. Use of extracellular matrix components for cell culture. *Anal Biochem* 1987;166:1–13.
38. Song E, Yeon KS, Chun T, Byun HJ, Lee YM. Collagen scaffolds derived from a marine source and their biocompatibility. *Biomaterials* 2006;27:2951–2961.
39. Chen G, Sato T, Ushida T, Hirochika R, Shirasaki Y, Ochiai N, Tateishi T. The use of a novel PLGA fiber/collagen composite web as a scaffold for engineering of articular cartilage tissue with adjustable thickness. *J Biomed Mater Res A* 2003;67:1170–1180.
40. O'Brien FJ, Harley BA, Yannas IV, Gibson LJ. The effect of pore size on cell adhesion in collagen-GAG scaffolds. *Biomaterials* 2005;26:433–441.
41. Kim HW, Li LH, Lee EJ, Lee SH, Kim HE. Fibrillar assembly and stability of collagen coating on titanium for improved osteoblast responses. *J Biomed Mater Res A* 2005;75:629–638.
42. Wahl DA, Sachlos E, Liu C, Czernuszka JT. Controlling the processing of collagen-hydroxyapatite scaffolds for bone tissue engineering. *J Mater Sci: Mater Med* 2007;18:201–209.
43. Thomas V, Dean DR, Jose MV, Mathew B, Chowdhury S, Vohra YK. Nanostructured biocomposite scaffolds based on collagen coelectrospun with nanohydroxyapatite. *Biomacromolecules* 2007;8:631–637.
44. Garcia AJ, Reyes CD. Bio-adhesive surfaces to promote osteoblast differentiation and bone formation. *J Dent Res* 2005;84:407–413.
45. Staatz WD, Fok KF, Zutter MM, Adams SP, Rodriguez BA, Santoro SA. Identification of a tetrapeptide recognition sequence for alpha 2 beta 1 integrin in collagen. *J Biol Chem* 1991;266:7363–7367.
46. Gilbert M, Giachelli CM, Stayton PS. Biomimetic peptides that engage specific integrin-dependent signaling pathways and bind to calcium phosphate surfaces. *J Biomed Mater Res* 2003;67:69–77.